ECTI Transactions on Computer and Information Technology
Journal homepage: https://ph01.tci-thaijo.org/index.php/ecticit/
Published by the ECTI Association, Thailand, ISSN: 2286-9131

Region Growing based K-means Clustering and Optimal Weight Prior-Attention Residual Learning for Segmentation and Classification of COVID-19 CT Images

D. Divya[1] and M. Thilagu[2]

ABSTRACT

COVID-19 has recently grown significantly over the globe, posing several obstacles for scholars. The first stage in COVID-19 and lung image analysis is lung image segmentation. Due to the intensity inhomogeneity, presence of artifacts, and proximity to the grey level of various soft tissues, the primary difficulties of segmentation algorithms were accentuated. However, the situation takes much more time than determining slice-by-slice to identify the lesions from volumetric chest CT images. Manual screening of COVID-19 using Computed Tomography (CT) images is arduous. The detection and type-classification sub-networks and the ultimately linked layers' learning weights are growing harder to select. Sole this issue, the proposed introduces Region Growing Based K-Means Clustering (RKMC) for segmentation—residual Learning with proposed Optimal Weight Prior-Attention Residual Learning (OWPARL) for classification of COVID-19 CT images. Stacking OWPARL blocks enables quick model construction and end-to-end multi-task loss training. Using lung scans of patients with and without pneumonia, one 3D-ResNet branch is particularly trained as a binary classifier to identify the lesion locations inside the lungs. The performance evolution metrics are precision, specificity, sensitivity, F-measure, and Area Under Curve (AUC) results compared to the RKMC+OWPARL procedure, which proposes greater correctness.

Article information:

Keywords: Lung CT Segmentation, Region Growing Based K-Means Clustering (RKMC), Optimal Weight Prior-Attention Residual Learning (OWPARL), COVID-19

Article history:
Received: September 26, 2023
Revised: November 9, 2023
Accepted: January 18, 2024
Published: February 10, 2024 (Online)

DOI: 10.37936/ecti-cit.2024181.254263

1. INTRODUCTION

Most nations in the globe have seen a fast spread of the new coronavirus pneumonia (COVID-19) infection. In clinical settings, once related to real converse transcriptase polymerase chain reaction (RT-PCR), computed tomography (CT) is a viable technique for greatly faster COVID-19 broadcast. However, discovering scratches from volumetric chest CT scans slice-by-slice requires a lot of time and effort, making screening COVID-19 manually from CT images challenging [1]. The signs of COVID-19 on CT scans are also comparable to those of other viral pneumonia, as seen in Figure 1, making it problematic to differentiate COVID-19 manually after further virus-related pneumonia.

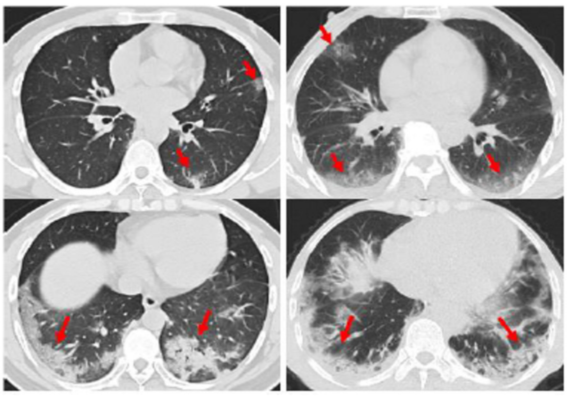

(a) COVID-19 (b) ILD

Fig.1: *Examples of (a) COVID-19 and (b) Interstitial Lung Disease (ILD) in CT Images.*

[1,2] The authors are with the Avinashilingam Institute for Home Science and Higher Education for Women, Coimbatore, India., Email: divyasnmv28@gmail.com and mthilagu@gmail.com

In consonance with the World Health Organization (WHO), Dehydration-related cough, exhaustion, and a running fever are symptoms of moderate and modest instances, whereas breathlessness and high temperatures along with weariness may occur in severe cases. People who already have illnesses, including respiratory disorders, diabetes issues, and heart conditions, are more susceptible to this virus and experience severe illness [2]. According to emerging evidence, those with significant lung disease are more likely to have brain damage due to hypoxia and/or pro-inflammatory mediators that connect the brain and lung. People are identified according to the indication and their travel history. One of these infections' most challenging aspects is that a person might have it for a long period without showing any symptoms. Most of the countries declared a partial or total lockdown for the whole impacted region due to its expanding nature and risk.

For developing networks capable of accurately simulating higher-order systems and reaching performance comparable to humans, the Deep Learning (DL) methodology is used. Since it will hasten diagnosis and improve access to treatment, creating a rapid, automated segmentation for COVID-19 infection is essential for illness evaluation. Due to the potent feature representation of DL technology, medical image processing has recently seen a significant increase with the fast growth of artificial intelligence [3-4]. To identify COVID-19 pneumonia from CT scans, many methods based on DL have been described.

Data availability for their identification and approximation ambiguity form the basis of conventional forecast accuracy. A rapid and accurate diagnosis will locate COVID-19, lessening the strain on medical providers. The diagnosis framework, which has a variety of aspects, was created to assist medical practitioners in prioritizing patients who need limited resources while also estimating the danger of infection. The objective is to create a model that can recognize COVID-19 since machine learning (ML) approaches are anticipated to be extensively employed in medical applications [5]. Predictive techniques connected to machine learning have proven useful in forecasting preoperative results to improve decision-making. Utilizing a set of training data that includes all of the COVID-19 characteristics, these systems are created [6]. To manage quick judgment and prevent the COVID-19 virus, predictive and exploratory characteristics of ML are thus essential.

In clinical practice, a trustworthy COVID-19 Computer-Aided Diagnosis (CAD) system should be helpful as it may reduce labor and improve the efficacy of detection by a physician. As illustrated in Fig. 1, pneumonia lesions in CT scans vary in size, morphology, and lung location, making system development problematic. Using just conventional ways to image processing or traditional methods of machine learning, both of which are dependent on manually-created descriptors, it seems challenging to create effective algorithms to manage the complex properties of pneumonia lesions.

Region Growing Based K-Means Clustering (RKMC) technique for segmentation. RKMC automatic pneumonia identification requires the crucial pre-requisite step of lung segmentation in CT images. It is a combined total of five lobes in the left and right human lungs. The chest and lungs are only two examples of the several segments that the CT image is split into. Identifying patterns of lung disease is focused on obtaining precise lung areas.

RKMC technique for segmentation and DL-based residual learning with the Optimal Weight Prior-Attention Residual Learning (OWPARL) is introduced for the classification of COVID-19 CT images in this work. Stacking the OWPARL blocks enables quick model construction and end-to-end multi-task loss training. With the use of lung scans of patients with and without pneumonia, one 3D-ResNet branch is particularly trained as a binary classifier to identify the lesion locations inside the lungs.

The main contribution of this research work:

- It is the COVID-19 screening using a deep learning algorithm.
- Region growing based K-Means Clustering (RKMC) and Optimal Weight Prior-Attention Residual Learning (OWPARL) algorithm is proposed to improve the overall prediction performance.
- Preprocessing, segmentation, and COVID-19 prediction are the key contributions of this study.
- With the use of efficient algorithms, the suggested technique produces more accurate findings for the provided dataset of lung CT images.

In Section 2, a literature survey of the research on COVID-19, ILD, and pneumonia has been done in terms of preprocessing, segmentation, and prediction approaches. The proposed methodology for RKMC algorithm and Optimal Weight Prior-Attention Residual Learning (OWPARL) scheme is detailed in Section 3. Section 4 contains a description of the experimental performance analysis findings. Last but not least, Section 5 summarizes the results.

2. RELATED WORK

Rustam *et al.* [7] proposed a Linear Regression (LR), Least Absolute Shrinkage and Selection Operator (LASSO), Support Vector Machine (SVM), and Exponential Smoothing (ES) for COVID-19 prediction. It explains how the number of persons who may contract COVID-19, which are now considered to be a threat to humans, can be predicted using machine learning techniques. In particular, COVID-19 for bidding factors is predicted using common predicting techniques as LR, LASSO, SVM, and ES. Forecasting over the next 10 days of three types, including the number of initially impacted cases, the number of fatalities, and the number of recovered cases. The study's findings showed that applying these methods to the current COVID-19 scenario is encouraging. It also showed that the ES technique, together with LR and LASSO, offers superior results in comparison to other methods, offering better prediction in detecting recently impacted patients, death rate, and recovered cases, but SVM offers lower performance in prediction. The evaluation metrics are R-squared (R^2) score, Adjusted R-square (R^2adjusted), Mean Square Error (MSE), Mean Absolute Error (MAE), and Root Mean Square Error (RMSE).

Zoabi *et al.* [8] a machine-learning technique was built and taught using data from 51,831 test subjects. Data from the next week's testing (47,401 tested people, of whom 3624 had COVID-19 confirmed) were included in the test set. Using just eight binary characteristics, our model accurately predicted the results of the COVID-19 test: intercourse, being older than 60 years old, showing the first five clinical indications, having had past contact with an infected individual, and Overall, a model that identifies COVID-19 instances by simple characteristics retrieved by asking fundamental questions was constructed based on the publicly disclosed national data from the Israeli Ministry of Health. The framework may prioritize COVID-19 testing when resources are scarce.

Barstugan *et al.* [9] proposed machine learning techniques Discrete Wavelet Transform (DWT), Local Directional Pattern (LDP), Grey Level Run Length Matrix (GLRLM), Grey Level Size Zone Matrix (GLSZM), Grey Level Co-occurrence Matrix (GLCM) ad Support Vector Machines (SVM) for early COVID-19 identification. Expert radiologists identified COVID-19's distinct behaviors from those of other viral pneumonia on the basis of CT imaging. Since early diagnosis of the COVID-19 virus is required, the clinical specialists clarify this. Using patches with sizes of 16x16, 32x32, 48x48, and 64x64 from 150 CT scans, four distinct datasets were created for the identification of COVID-19. Patches were exposed to the feature extraction approach in order to enhance the classification process. DWT, LDP, GLRLM, GLSZM, and GLCM as feature extraction methods. The collected characteristics were categorized using SVM. Cross-validations that were repeated two, five, and 10 times were employed throughout the categorization process. The effectiveness of the classification procedure was evaluated using sensitivity, specificity, accuracy, precision, and F-score metrics. Using the 10-fold cross-validation technique with the GLSZM feature extraction approach, the highest classification accuracy was attained at 99.68%.

Pahar *et al.* [10] developed, using COVID-19 cough data from a smartphone, a machine learning-based classifier that can distinguish between healthy, unhealthy, and positive coughs. A cross-validation scheme was used to train and evaluate seven machine learning classifiers: Logistic Regression (LR), K-nearest Neighbour (KNN), Support Vector Machine (SVM), Multilayer Perceptron (MLP), Convolutional Neural Network (CNN), Long Short-Term Memory (LSTM) and a Residual-based Neural Network Architecture (Resnet50).This non-contact screening strategy advises patients with COVID-19-related coughs to self-isolate early, which may reduce testing centers' workload. Since both forced and natural coughs were included in the datasets utilized, it can be concluded that the method is broadly applicable. 18 COVID-19 positive and 26 smaller datasets, COVID-19 negative people who had a SARS-CoV laboratory test are included in the second; it was mostly compiled in South Africa. There are 1079 healthy individuals and 92 persons who tested positive for COVID-19 in the publicly available Coswara dataset. COVID-19-positive coughs are 15% -20% shorter than non–COVID coughs, according to both datasets. Results show that although all classifiers were able to identify COVID-19 coughs, the best performance was exhibited by the Resnet50 classifier, which was best able to discriminate between the COVID-19 positive and the healthy coughs with an area under the ROC curve (AUC) of 0.98. LSTM classifier was best able to discriminate between the COVID-19 positive and COVID-19 negative coughs, with an AUC of 0.94 after selecting the best 13 features from a sequential forward selection (SFS). Since this type of cough audio classification is cost-effective and easy to deploy, it is potentially a useful and viable means of non-contact COVID-19 screening.

Xu *et al.* [11] introduced a unique technique that uses deep learning technology to automatically evaluate COVID-19 CT images. A model with a location-attention mechanism that has an overall accuracy rate of 86.7% and can classify COVID-19, IAVP, and healthy patients might be used as an additional diagnostic tool by front-line clinical practitioners. Identifying pixel-level masks for pneumonia lesion areas is quite challenging. Additionally, complicating this endeavor was the lesion locations' inconsistent 3D architecture. Thus, this segmentation procedure resembled object-detection algorithms. Professional radiologists confirmed the model's suitability to distinguish candidate patches for viral pneumonia even though it was developed for the aim of detecting pulmonary TB.

Shi *et al.* [12] emphasized the significance of quickly and properly diagnosing COVID-19 from community-acquired pneumonia (CAP) in patients. 1,658 individuals with COVID-19 and 1,027 patients with CAP were all included in this research and received thin-section CT. To acquire the lung fields and infection segmentations, all images underwent pre-processing. To better capture the COVID-19 dispersion pattern, a set of bespoke location-specific variables is used in place of the conventional CT severity score (CT-SS) and radionics characteristics. An infection size-aware random forest approach (iSARF) separates COVID-19 from CAP. According to experimental findings, the technique performed best when employing handmade features, outperforming state-of-the-art classifiers in terms of accuracy, specificity, and sensitivity by 90.7%, 87.2%, and 89.4%, respectively. With thick slice images, further tests on 734 participants show excellent generalizability. The framework may help with clinical decision-making, it is hoped.

Khan *et al.* [18] proposed three Convolution Neural Networks (CNNs) for identifying the cause (either due to COVID-19 or other types of infections) of pneumonia from radiology images. Furthermore, because different variants of COVID-19 lead to different patterns of pneumonia, the proposed methodology identifies pneumonia, COVID-19-caused pneumonia, and Omicron-caused pneumonia from the radiology images. To fulfill the above-mentioned tasks, we have used three Convolution Neural Networks (CNNs) at each stage of the proposed methodology. The results unveil that the proposed step-by-step solution enhances the accuracy of pneumonia detection along with finding its cause despite having a limited dataset. The performance evaluation metrics are Accuracy, Specificity, Sensitivity, Cohen's kappa, and Standard deviations. The pneumonia-positive case is discriminated against the COVID-19 case with 87% accuracy. The COVID-19 identified case is discriminated against Omicron-caused pneumonia with 78% accuracy. These accuracy levels are achieved with twenty training epochs. The radiology images can be successfully used for the identification of pneumonia with high accuracy along with the identification of COVID-19 and Omicron variant-caused pneumonia with reasonable accuracy.

3. RESULTS AND DISCUSSION

This study proposes the use of the Optimal Weight Prior-Attention Residual Learning (OWPARL) method and the RKMC algorithm to enhance COVID-19 prediction performance. The proposed system contains three main phases: noise removal, segmentation, and classification. The noise removal is done by using the Adaptive Median Filtering (AMF) algorithm to reduce the noise data from the given CT lung image database. It is used to increase the classification accuracy more effectively. It is mostly used to provide a solid and practical model for enhancing image outcomes when there is a lot of noise present. These features are taken into the segmentation process for obtaining more informative features from the CT image database. It is performed by using the RKMC algorithm, and it is used to compute the necessary and prominent features based on the centroid values. Automatic pneumonia identification requires the crucial pre-requisite step of lung segmentation in CT images. Finally, the OWPARL algorithm is applied for classification through training and testing models. It classifies the COVID features more accurately using weight values. With the use of lung scans of patients with and without pneumonia, one 3D-ResNet branch is particularly trained as a binary classifier to identify the lesion locations inside the lungs. The effectiveness of COVID-19 images may be greatly improved, according to experimental findings, which support the suggested framework. The experimental result proves that the proposed OWPARL algorithm provides better classification performance than the existing algorithms in terms of higher AUC, precision, sensitivity, specificity, f-measure, and accuracy.

3.1 Dataset Collection

The dataset has 2482 SARS-CoV-2 CT images, of which 1252 test positive for the virus (COVID-19) and 1230 test negative. Real patients from Sao Paulo, Brazil's hospitals, provided the data for this study. By analyzing an individual's CT scans, the objective of this dataset is to further research into and create machine learning methods for detecting SARS-CoV-2 infection. The images were gathered from studies published in journals like NEJM, JAMA, Lancet, and bioRxiv connected to COVID-19. Reading the figure captions in the studies helps us choose the CTs that have COVID-19 anomalies. Figure 2 depicts the system's suggested overall processing flow diagram.

3.2 Noise Removal Using Adaptive Median Filter (AMF) on CT Images

Noise is a random shift in image intensity that may be perceived as part of the grains. The study of anatomical structure and image processing for medical images needs the use of noise reduction methods, which have become a vital practice. Noise reduction algorithms eliminate image noise. Noise reduction methods smooth the overall image, leaving contrast-limited zones. This decreases noise appearance. There are several noise removal algorithms. Consider, for the purpose of noise elimination, the concepts of the mean and the adaptive median filter. Mean filtering is a way of smoothing images that is relatively easy to apply; nevertheless, it is quite sluggish, and the noise removal is fully effective in increasing the correctness of the model.

Noise reduction is carried out in this study by utilizing the AMF method, which is focused on removing extra noise from the provided CT images. It is mostly used to provide a solid and practical model for enhancing image outcomes when there is a lot of noise

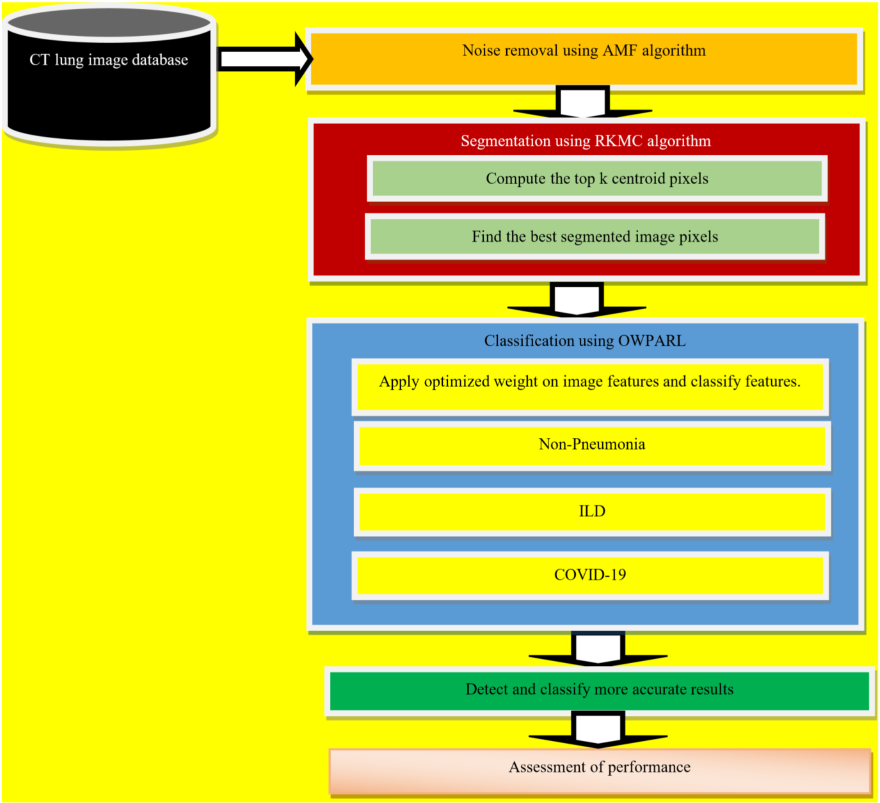

Fig.2: *The Proposed System Flow.*

present. The main reason for using AMF method (1) establishes which pixels in an image have been impacted by noise, AMF conducts spatial processing [13], (2) Each pixel in the image is evaluated in relation to its immediate neighbors by the AMF before being classified as noise, (3) Adjustable parameters include the neighborhood's size and the comparison threshold [14], (4) Noise is defined as a pixel that is architecturally out of alignment with its like pixels and distinct from most of its neighbors, (5) Finally, surrounding pixels that passed the noise identification test are used to replace the noise pixels with their median pixel values. In order to increase image quality, noise in the image is reduced.

The window size of an adaptive filter increases as the number of noise candidates increases in a specific region. The amount of noisy pixels in each region is used in a calculation to estimate the window size (1). Following thorough simulations that ensure the optimum outcomes for modifying window size in accordance with the quantity of noisy pixels in an area, Mean Square Error (MSE) parameters are specified.

$$W(M) = \sum_{p} C(p, D_p) + \sum_{q\epsilon N_p} T\left[|M_p - M_q = 1\right] + \sum_{q\epsilon N_p} T\left[|M_p - M_q > 1\right] \tag{1}$$

The window matching function is denoted by W, while W's ideal solution is denoted by M. The real pixel in the displayed image is pixel p, while pixel q is pixel's neighbor. Stands for the group of pixels that are close to p. M_P and, M_q, respectively, are the estimated matched windows for p and q. C stands for a certain matching window's price. $T[\cdot]$ is a logical function that examines the statements it contains, determines whether or not those statements are true, and then returns one if they are true and 0 otherwise. If there are no noise-free pixels and the median is noisy (1), increase the window size in the calculation. If the predefined conditions are not met, the image pixel filter window size grows. The window's median filters the pixel if the criteria are met. I_{med} is the median of the allotted window, and W_{max} is the largest window size that may be attained. Let I_{ij} be the corrupted image's pixel, I_{min} be its minimum pixel value, I_{max} be its maximum pixel value, and W be the window's current size. Below are the two levels of this filtering approach.

Level A:

a) If $I_{min} < I_{med} < I_{max}$, the median value is thus not noise. In order to assess whether the current pixel is noise, the model moves on to Level B.

b) In the event that this is not the case, the window size is increased using equation (1), and Level A continues until the median value is no longer noisy, at which time the model shifts to Level B. If the maximum window size is reached, the median value is utilized as the value for the filtered image pixel.

Level B:

a) If $I_{min} < I_{ij} < I_{max}$, the pixel in the filtered image is constant because the current value of that pixel is not noise.

b) If, however, either the image pixel's value I_{max} or I_{min} (corrupted), Afterward Each pixel of the filtered image is given the Level A median value.

The proposed method of adaptive median filter compared with mean filter output is shown in Figure 3. Based on the experimental results, the adaptive median filter produces better noise removal than the mean filter algorithm. Figure 3 shows the difference between the mean filter and the proposed AMF image. It shows that the proposed AMF removes the noise more effectively than the mean filtering approach.

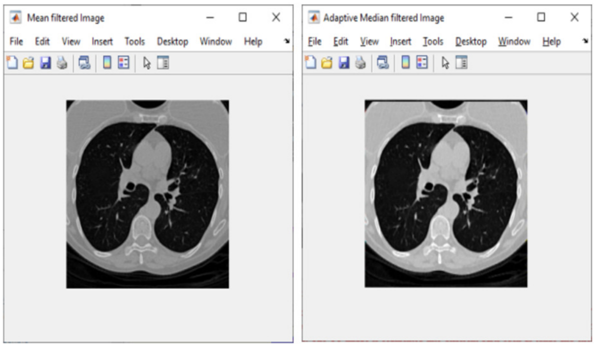

Fig.3: *Preprocess Image Comparison of the Proposed System.*

3.3 RKMC Algorithm for Segmentation

In this study, the RKMC algorithm is effectively used for image segmentation. Automatic pneumonia identification requires the crucial pre-requisite step of lung segmentation in CT images. There is a combined total of five lobes in the left and right human lungs. The chest and lungs are only two examples of the several segments that the CT image is split into. Identifying patterns of lung disease is focused on obtaining precise lung areas. It is still a challenging technique because of the amorphous form and fuzzy edges of lung tissues. Obtaining a chest regional mask that also removes the inner cavities is the first step in segmenting the lung regions.

Based on the initial centroids of clusters, KMC is a powerful clustering approach for classifying comparable data into groups.To determine the cluster centroids, it makes use of the Euclidean distance notion. The black and white images are divided up by RKMC. In this study, COVID-19 is more accurately predicted by early diagnosis of illness using CT scans. The technique continually partitions a space at random. (i) the current cluster centers are calculated, and (ii) provides the nearest center for each piece of information in the cluster. Reassignments stop it. This method reduces intra-cluster variance, differences between data attributes and cluster nodes, expressed as the square root of their sum.

Since it includes choosing to start seed points, the technique is known as pixel-based image segmentation. Using initial seed points as a starting point, this segmentation method looks at the surrounding pixels to see whether they should be included in the segmented area. Iterative techniques include region splitting and region merging. In order to get a suitable segmented image of the original image, region splitting is often performed on an image first in order to separate it into the largest number of regions. In the same location, it is hypothesized that adjacent pixels should have equal intensity levels. An example of the KMC algorithm is shown in Figure 4.

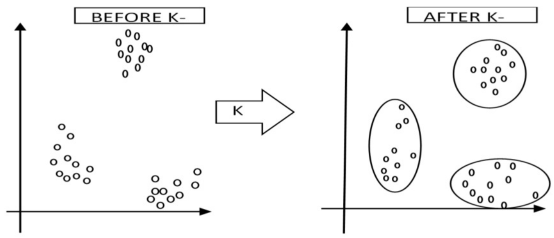

Fig.4: *Example of KMC Algorithm.*

K-means implementation is very useful because of its effectiveness and simplicity. The number of classes and the number of clusters are unaltered in this investigation. The Euclidean distance may be calculated using the formula below, and cluster centroids can be located using it.

$$d(i,j) = \sqrt{\sum_{i=1}^{n}(x_i - y_i)^2} \tag{2}$$

When there are two points in Euclidean n-space, x_i and y_i.

Algorithm 1: RKMC algorithm

1. From the CT image database, choose k clusters (D)
2. Initialize cluster centers $\mu 1, \ldots \mu k$ and segment the images
3. Choose k data points, align cluster centers with these points, and then extract beginning seeds from the clusters.
4. Find the nearest pixels after randomly allocating points to clusters and calculating their means.
5. To calculate the distance between values, use the cluster center that is closest to each data point.
6. Using (2), determine the minimum distance pixels and check the area expanding pixels.
7. Assign the data point to this cluster by comparing the similarity of the pixels, then updating the

nearest existing area that is tied to the seed.
8. Re-compute cluster centers and find the affected tissues in the given images
9. Identify the earlier prediction probability of COVID-19 images
10. When no fresh re-assignments are received, stop

On the whole database set, the RKMC method is used to produce clusters of full pixels. The pixels are taken one by one, and their prospective values are used to fill the region-based pixels. The CT lung images, it is mostly utilized to diagnose the earliest stage of COVID illness. Based on the afflicted markings, it first divides the lung area images. It is applied to locate the expected pneumonia lesions' segments. The earlier illness probability across the provided CT image was effectively taken into account by the RKMC algorithm in this study. After RKMC is applied to the CT lung image database from the created clusters, the newly added pixels are evaluated for proper classification. In the event that it is situated inside the suitable cluster, the value that has been given to it will be made permanent, and the process will then go on to the next set of pixels [15]. The next feasible value will be assigned and compared until the value that places the pixels in the proper cluster is discovered if it is in the incorrect cluster. As a result, the accuracy of the classifier and the prediction of early pneumonia are both improved in this study. Additionally, the RKMC approach is utilized to raise COVID-19 classification accuracy in cases where pneumonia or ILD would otherwise occur.

3.4 Classification via Optimal Weight Prior-Attention Residual Learning (OWPARL) Algorithm

In this work, classification is performed by using the Optimal Weight Prior-Attention Residual Learning (OWPARL) algorithm. A branch for the duty of detecting pneumonia and a branch for the task of classifying types are included in each PARL block.

We crop the refined lung areas in accordance with the lobe mask after the lobe mask has been obtained. The picture is then cropped and shrunk to 96 x 96 x 96 before being put into the 3D-ResNets to forecast pneumonia.

Pneumonia identification and pneumonia-type classification are two tasks that two 3D-ResNet-based sub-networks are intended to perform, as illustrated in Figure 5. The detection sub-network classifies CT scans for pneumonia, whereas the type-classification sub-network classifies ILD and COVID-19. To enhance COVID-19 screening, a prior-attention strategy closely integrates the two sub-networks convolutional layers. The process of inference may be stated as follows:

$$P = f(I, W_{det}, W_{cls}|S(W_{det}, W_{fc} \tag{3}$$

where f, W_{det}, and W_{cls} denote the sub-networks learned convolutional weights, respectively, and I denote the volumetric lung image supplied into the model. The fully connected layers' learning weights are denoted by $W_{fc}.S(\cdot)$ a function of attention. A softmax probability vector, or the output P, is produced.

$$P = \left[p^{non}, p^{ILD}, p^{COVID}\right] \tag{4}$$

where p^{non},p^{ILD}, and p^{COVID} are the three categorization groups' associated probabilities, in that order.

The non-lesion regions of the lung areas on a CT image often make up a significant portion of the lung regions and are home to complex variations of the lung tissues, such as arteries and fibers. The type-classification is negatively affected by these non-lesion areas. We use the detection sub-networks convolutional feature maps to build soft lesion-aware maps to solve this problem. The type-classification sub-network is then given the soft maps to have it focus on the lesion locations. We refer to this information as "prior attention" since it is produced by a different model than the type-classification model itself.

In actuality, it is possible to train both sub-networks separately. The training process begins with the training of the detection sub-network, followed by the training of the type-classification sub-network, and ultimately, the fully connected layer, which integrates the output of the two sub-networks. There are two major problems with this training approach, however. First, compared to end-to-end training, multi-stage training takes much more. The prior-attention mechanism, which moves the attention information from a detection model that has already been trained to a type-classification model, is difficult to implement, according to the second point. In order to enable the transmission of hierarchical prior-attention information within the basic blocks, we merged the prior-attention process into a novel residual learning block. By cascading the blocks and employing multi-task loss, the suggested modular network architecture makes it simple to construct deep attention models.

Each PARL block, as seen in Figure 4, has two branches: one for the purpose of detecting pneumonia and the other for the duty of classifying types.

Three stacked 3D convolutional layers, a "shortcut connection," and an "attention connection" are included in the classification branch's prior-attention residual learning unit. The underlying mapping of the convolutional layers and the shortcut connection is appropriate for the attention connection, and $\sigma^2(x_2), \alpha(x_1, x_2)$, and $h^2(x_2, W_2)$ the unit's output may be stated as follows, respectively:

$$f^2(x_2) = \sigma^2(x_2) + h^2(x_2, W_2) + \gamma \times \alpha(x_1, x_2) \tag{5}$$

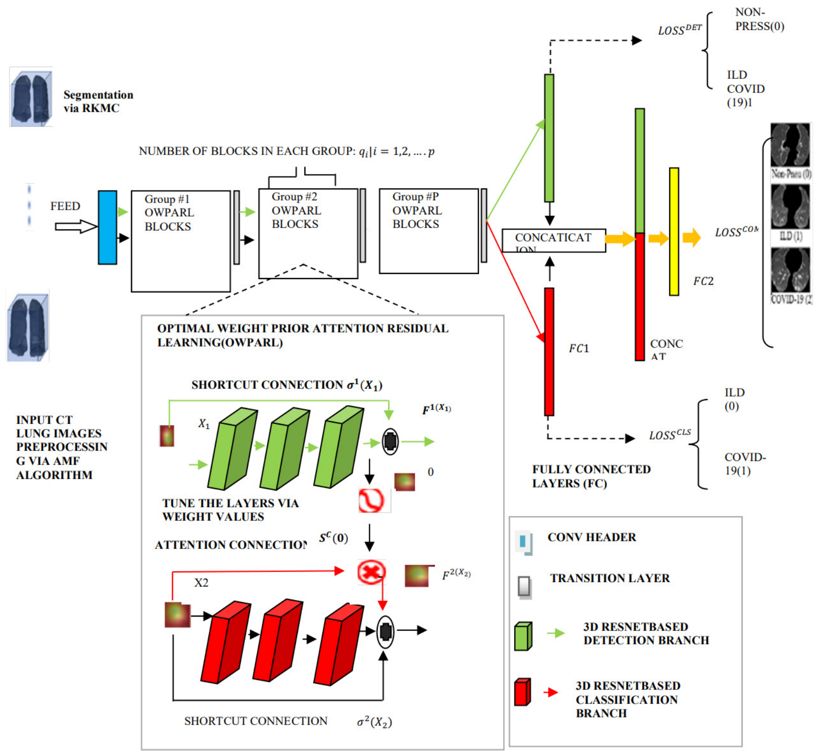

Fig.5: *The Architecture of the Proposed RKMC+OWPARL System.*

where x_2, W_2 represent, in the classification branch, the convolutional layers' learnt weights and the unit's input feature map, respectively. x_1 is the residual unit's detection branch's input feature map. γ The weighting factor controls the attention feature map's trade-off with the other two feature maps. For the purpose of simplicity, in our implementation, γ is set to 1.0 by default. The brief connect can simply be implemented as an identity mapping, according to the original residual learning [16].

$$\sigma^2(x_2) = x_2 \tag{6}$$

The crucial element in (3) to enhance the classification performance is the attention link $\alpha.(x_1, x_2)$. To create a soft attention map, the input feature map is multiplied by each element.

$$\alpha(x_1, x_2) = S(O).x_2 \tag{7}$$

where $O = h^1(x_1)$, the detection branch's final layer's feature maps are presented. The term of $S(\cdot)$ normalizes the feature map to create the soft attention map **O**

$$S(O) = \left\{ m | m^c_{i,j,k} = \frac{e^{O^c_{i,j,k}}}{\sum_{i',j',k'} e^{O^c_{i,j,k}}} \right\} \tag{8}$$

where i, j, k a, and indicate channel index and location. Coordinates **O**, respectively. $S(\cdot)$ highlights critical detects using a spatial softmax function.

To regularize the dropout, the penultimate layer is weighted (13) states it,

$$y = w.z + b \tag{9}$$

The equation is used to produce the output y in forward propagation, dropout (14),

$$y = w.(z \circ r) + b \tag{10}$$

Here $\circ$ element-wise multiplication operator represented and $r \in \mathbb{R}^m$, the Bernoulli random variable "masking" vector with probability p = 1. Unmasked units propagate gradients. The weight vectors are scaled by p during testing $\hat{w} = pw$, and $\hat{w}$ enables the creation of hidden samples. As well as that, by rescaling w to incorporate the weight vectors' l_2-norms $||w||_2 = s$ when $||w||_2 > s$ after a step of incline decline.

Softmax layer or fully connected layers are excellent at formatting multi-class probabilities, nevertheless, within limits. Hence, ReLU is employed as an activation function. ReLU definition is demonstrated in equation (15),

$$f(x) = \begin{cases} 0 \,, if \quad x < 0 \\ x \,, if \quad x \geq 0 \end{cases} \tag{11}$$

N neurons connected to N feature classes make up the output layer. The layer below is completely linked. In the standard approach, the provided input is classified using the high-output neuron as the class label. It classifies whether the given feature is Non-Pneumonia, ILD, or COVID-19 more accurately.

4. EXPERIMENTAL RESULTS

The input image is taken from the following links [19] [20]. The performance metrics are considered, such as accuracy, specificity, sensitivity, precision, F-measure, and Area Under Curve (AUC), and it is evaluated using existing Random Forest(RF)[17], Prior-Attention Residual Learning(PARL) and proposed RKMC+ OWPARL algorithms.

Table 1: *Comparison Values of Existing and Proposed Methods.*

	Methods		
Performance Metrics	**RF**	**PARL**	**RKMC+OWPARL**
Accuracy	87	93	95
Precision	79	88	92
Sensitivity	97	90	93
Specificity	86.3	95.5	96.77
F-measure	80	85	89
AUC	84	87	93

Table 1 shows the comparison values of existing and proposed methods. The RKMC+OWPARL method is more accurate than the RF and PARL algorithms for the CT lung image database. Preprocessing is used to improve detection and classification accuracy through the use of the AMF algorithm. The proposed lung lobe region-based segmentation improves pixel strength using the RKMC algorithm.RKMC is focused on combining relevant information from segmented CT lung images, which are more informative. It also extracts more relevant information that belongs to non-pneu, ILD, or COVID-19. Hence, the proposed RKMC+OWPARL provides higher accuracy, precision, sensitivity, specificity, f-measure, and AUC values than the existing RF and PARL methods.

Accuracy

The sum of the classification parameters (T_p+T_n+F_p+ which are divided by the total number of actual classification parameters (T_p+T_n), are calculated to assess accuracy, which is defined as the model's overall correctness.

This is how the accuracy is calculated:

$$\text{Accuracy} = \frac{T_p + T_n}{(T_p + T_n + F_p + F_n)} \tag{12}$$

where Fp is for false positive, Fn is for false negative, Tp is for true positive, Tn is for true negative.

The existing and recommended methods are used to evaluate the comparison measure's accuracy, as shown in Figure 6. The y-axis represents the accuracy value, while the x-axis represents the techniques. The RKMC+OWPARL method is more accurate than the RF and PARL algorithms for the CT lung image database. Preprocessing is used to improve detection and classification accuracy through the use of the AMF algorithm. The proposed lung lobe region-based segmentation improves pixel strength using the

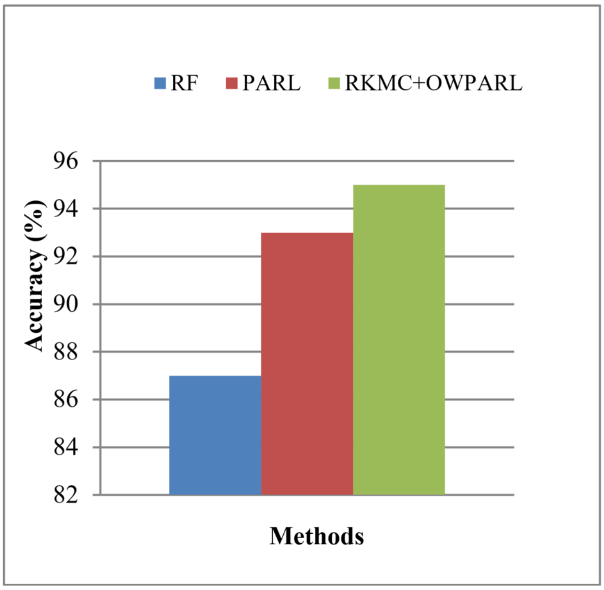

Fig.6: *Performance with Accuracy.*

RKMC algorithm. Thus, the result concludes that the proposed RKMC+OWPARL algorithm increases the COVID-19 screening performance through the optimized weight values in fully connected layers.

Specificity

The percentage of genuine negatives that are accurately classified as such is a measure of specificity.

$$\text{Specificity} = \frac{T_n}{T_n + F_p} \tag{13}$$

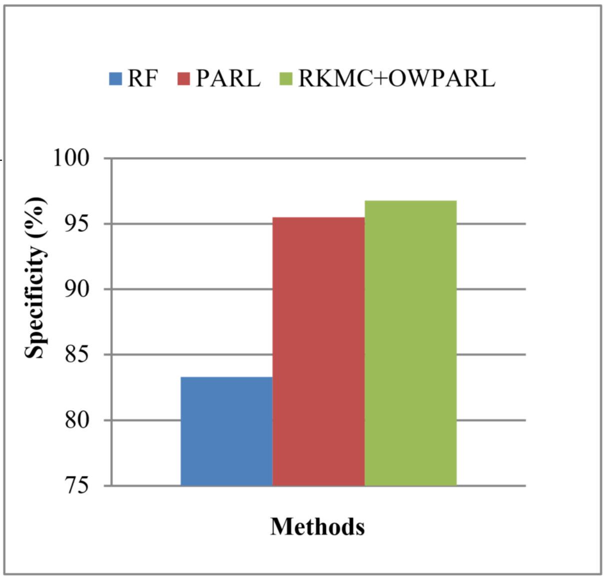

Fig.7: *Performance with Specificity.*

The comparison measure is assessed for specificity using the techniques that are currently in use, as can be seen from Figure 7 mentioned above. In the y-axis, the specificity value is shown, and the techniques are used for the x-axis. The proposed RKMC+OWPARL method provides higher specificity, whereas existing RF and PARL methods provide lower specificity. The proposed RKMC is focused on combining relevant information from segmented CT lung images, which is more informative. Thus, the result concluded that the proposed RKMC+OWPARL approach increases the image features accurately for the COVID-19 detection and classification process.

Sensitivity

The percentage of genuine positives that are correctly classified as such in certain disciplines is known as the true positive rate, recall, or probability of detection.

$$\text{Sensitivity} = \frac{T_p}{T_p + F_n} \tag{14}$$

Fig. 8 illustrates how the comparison metric's sensitivity is measured. The y-axis shows the sensitivity value, while the x-axis shows the approaches. The proposed RKMC+OWPARL method provides higher sensitivity, whereas existing RF and PARL methods provide lower sensitivity. The proposed RKMC is focused on combining relevant information from segmented CT lung images, which is more informative. Thus, the result concluded that the proposed RKMC+OWPARL approach increases the image features accurately for COVID-19 detection and classification process.

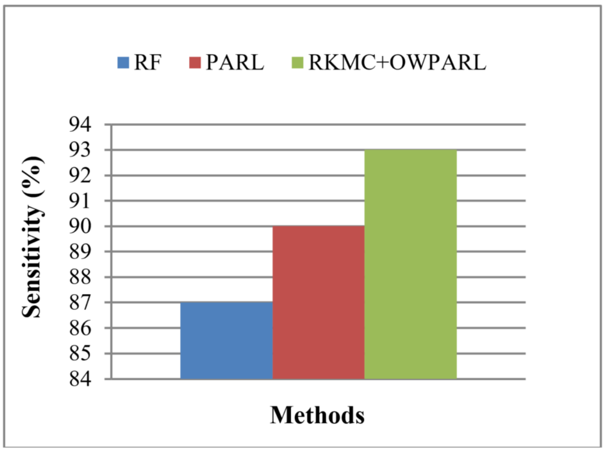

Fig.8: *Performance with Sensitivity.*

Fig. 8 illustrates how the comparison metric's sensitivity is measured. The y-axis shows the sensitivity value, while the x-axis shows the approaches. The proposed RKMC+OWPARL method provides higher sensitivity, whereas existing RF and PARL methods provide lower sensitivity. The proposed RKMC is focused on combining relevant information from segmented CT lung images, which is more informative. Thus, the result concluded that the proposed RKMC+OWPARL approach increases the image features accurately for COVID-19 detection and classification process.

Precision

$$\text{Precision} = \frac{T_p}{T_p + F_p} \tag{15}$$

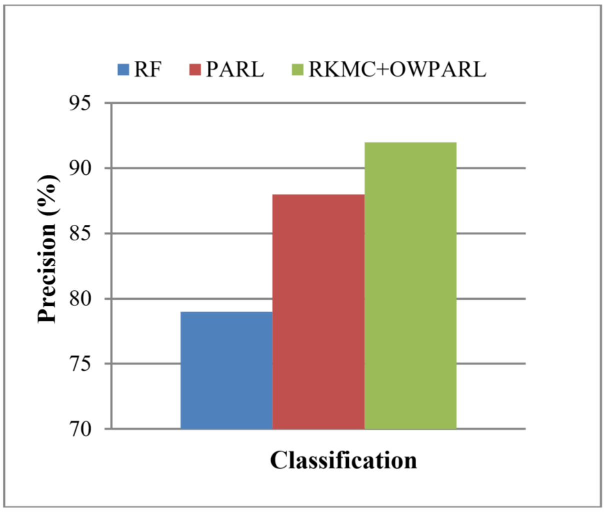

Fig.9: *Performance with Precision.*

Precision and recall are both measures of accuracy or quality. High accuracy means an algorithm produces a high proportion of relevant results. A classification task's accuracy is determined by dividing the number of real positives by the total objects categorized as positive.

The comparison measure is assessed using both the present and suggested technique in terms of accuracy, Figure 9 shows. The y-axis shows accuracy, while the x-axis shows methods. The suggested RKMC+OWPARL algorithm gives greater accuracy for the supplied CT lung images as compared to the current approaches, which, for example, the RF and PARL algorithms, provide lesser precision. The proposed method improves the precision through the extraction of more relevant information that belongs to non-pneu, ILD, or COVID-19. In this work, RKMC segments the images efficiently via centroid values. As a consequence, the analysis's findings show that the suggested RKMC+OWPARL algorithm improves COVID-19 classification performance via the use of the most effective segmentation technique.

F-measure

F1-score is defined as:

$$\text{F1-score} = \frac{2 \times \text{precision} \times \text{recall}}{\text{precision} + \text{recall}} \tag{16}$$

Evaluation of the comparative values for the proposed and current algorithms for the F-measure metric is done in Figure 10. The suggested RKMC+OWPARL technique delivers a greater F-measure for the provided CT lung image database than the current RF and PARL approaches, which produce a lower F-measure. Without any characteristics that were improperly recognized, the suggested

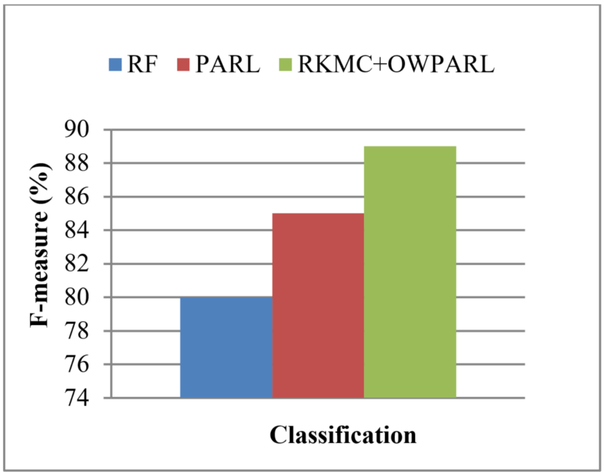

Fig.10: *Performance with F-measure.*

RKMC+OWPARL classifier showed that the prediction had an F1 score of 92%. RKMC algorithm is used to provide optimal segmentation results. As a result, the proposed RKMC+OWPARL algorithm offers improved COVID-19 detection performance for the CT lung image database and greater classification accuracy.

AUC

AUC uses a curve known as the receiver operating characteristic (ROC) curve. When a binary classifier's discriminating threshold is changed, the TPR versus the FPR is graphically shown on the ROC-curve.

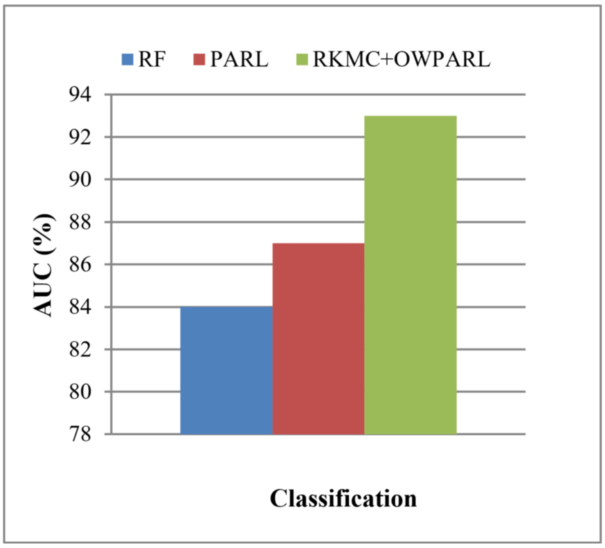

Fig.11: *Performance with AUC.*

As shown in the aforementioned Figure 11, the present and recommended techniques evaluate the comparison measure's AUC. The x-axis shows approaches, while the y-axis shows AUC. The RKMC+OWPARL method outperforms the RF and PARL algorithms on the CT lung image database. Through the use of the AMF algorithm, the preprocessing improves the detection and classification accuracy. The RKMC method strengthens pixels using the suggested lung lobe region-based segmentation. According to the results, due to the adjusted weight values in fully connected layers, the suggested RKMC+OWPARL algorithm improves the COVID-19 screening performance.

Confusion Matrix

A confusion matrix represents the prediction summary in matrix form. It shows how many predictions are correct and incorrect per class. It helps in understanding the classes that are being confused by the model as other classes. Confusion matrix is shown in table 2.

Table 2: *Confusion Matrix.*

Actual classes			
	0	1	2
Predicted classes			
0	48.0	1.0	0.0
1	1.0	49.0	6.0
2	1.0	0.0	44.0
	Actual classes		
True Positive	48.00	49.00	44.00
False Positive	1.00	7.00	1.00
False Negative	2.00	1.00	6.00
True Negative	99.00	93.00	99.00
Precision	0.97	0.86	0.97
Recall or sensitivity	0.97	0.99	0.89
Specificity	0.98	0.92	0.98

Through the confusion matrix, the proposed RKMC+OWPARL system provides better classification results for the given dataset.

5. ADVANTAGES AND DISADVANTAGES OF PROPOSED WORK

Advantages of proposed work:

1. OWPARL algorithm, which provides more accurate classification performance.
2. The new approach offers superior accuracy, precision, specificity, sensitivity, F-measure, and AUC.

Disadvantages of proposed work:

1. It is not suitable for larger datasets.
2. It is a time.
3. Not focused on feature extraction, the algorithm can be developed for multi-modality images

6. CONCLUSION AND FUTURE ENHANCEMENT

The RKMC+OWPARL method is suggested in this study to enhance the COVID-19 detection and classification performance for the supplied CT lung images. The four essential components of this study are COVID-19 classification, segmentation, and noise reduction. The performance of COVID-19 screening, ILD, and pneumonia classification are improved by employing the AMF algorithm to remove noise. Then CT lung images are segmented via RKMC algorithm. It segments the images that were used for earlier predictions of COVID-19 and pneumonia. Lesion locations throughout the lungs are highlighted using a 3D-ResNet branch that has been trained as a binary classifier using lung images with and without pneumonia. Classification is done by using the OWPARL algorithm, which provides more accurate classification performance. When comparing the suggested RKMC+OWPARL method to the current algorithm, it was found that the new approach offers superior accuracy, precision, specificity, sensitivity, F-measure, and AUC.

Future Enhancement

1. In future work, hybrid soft computing algorithms and feature extraction algorithm can be developed for multi-modality images.
2. Recent Optimization-based algorithms are used to support larger datasets and also improve classification accuracy.

References

[1] X. Zhao, B. Liu, Y. Yu, X. Wang, Y. Du, J. Gu and X. Wu, "The characteristics and clinical value of chest CT images of novel coronavirus pneumonia," *Clinical radiology*, vol. 75, no. 5, pp.335-340, 2020.

[2] K. Simonyan and A. Zisserman, "Very deep convolutional networks for large-scale image recognition," *Published as a conference paper at ICLR 2015*, pp.1-14, 2014.

[3] S. Ren, K. He, R. Girshick and J. Sun, "Faster R-CNN: Towards real-time object detection with region proposal networks," *Advances in neural information processing systems*, vol. 28, pp.1-9, 2015.

[4] T. Y. Lin, P. Dollár, R. Girshick, K. He, B. Hariharan and S. Belongie, "Feature pyramid networks for object detection," *Proceedings of the IEEE conference on computer vision and pattern recognition*, pp. 2117-2125, 2017.

[5] S. Kushwaha *et al.*, "Significant applications of machine learning for COVID-19 pandemic," *Journal of Industrial Integration and Management*, vol. 5, no. 4, pp. 453-479 , 2020.

[6] D. Goodman-Meza *et al.*, "A machine learning algorithm to increase COVID-19 inpatient diagnostic capacity," Plos one, vol. 15, no. 9, pp. 1-10, 2020.

[7] F. Rustam *et al.*, "COVID-19 Future Forecasting Using Supervised Machine Learning Models," in *IEEE Access*, vol. 8, pp. 101489-101499, 2020.

[8] Y. Zoabi, S. Deri-Rozov and N. Shomron, "Machine learning-based prediction of COVID-19 diagnosis based on symptoms," *npj digital medicine*, vol. 4, no. 1, pp. 1-5, 2021.

[9] M. Barstugan, U. Ozkaya and S. Ozturk, "Coronavirus (covid-19) classification using ct images by machine learning methods," *arXiv preprint arXiv:2003.09424*, pp. 1-10, 2020.

[10] M. Pahar, M. Klopper, R. Warren and T. Niesler, "COVID-19 cough classification using machine learning and global smartphone recordings," *Computers in Biology and Medicine*, vol. 135, pp. 1-10, 2021.

[11] X. Xu *et al.*, "A deep learning system to screen novel coronavirus disease 2019 pneumonia," *Engineering*, vol. 6, no. 10, pp. 1122-1129, 2020.

[12] F. Shi *et al.*, "Large-scale screening to distinguish between COVID-19 and community-acquired pneumonia using infection size-aware classification," *Physics in medicine & Biology*, vol. 66, no. 6, pp. 1-7, 2021.

[13] K. Verma, B. K. Singh and A. S. Thoke, "An enhancement in adaptive median filter for edge preservation," *Procedia Computer Science*, vol. 48, pp. 29-36, 2015.

[14] H. Ibrahim, N. S. Pik Kong and T. F. Ng, "Simple adaptive median filter for the removal of impulse noise from highly corrupted images," in *IEEE Transactions on Consumer Electronics*, vol. 54, no. 4, pp. 1920-1927, November 2008.

[15] A. A. A. Setio *et al.*, "Validation, comparison, and combination of algorithms for automatic detection of pulmonary nodules in computed tomography images: the LUNA16 challenge," *Medical image analysis*, vol. 42, pp.1-13, 2017.

[16] A. Ter-Sarkisov, "Covid-ct-mask-net: Prediction of covid-19 from ct scans using regional features," *Applied Intelligence*, vol. 52, no. 9, pp. 9664-9675, 2022.

[17] C. Iwendi *et al.*, "COVID-19 patient health prediction using boosted random forest algorithm," *Frontiers in public health*, vol. 8, no. 357, pp.1-9, 2020.

[18] A. A. Khan *et al.*, "Detection of Omicron Caused Pneumonia from Radiology Images Using Convolution Neural Network (CNN)," *Computers, Materials & Continua*, vol. 74, no. 2, pp. 3743–3761 , 2023.

[19] `https://www.kaggle.com/plameneduardo/sarscov2-ctscan-dataset?select=non-COVID`

[20] `https://www.kaggle.com/luisblanche/covidct.`

D. Divya has completed M.Sc. B.Ed., M.Phil. in Computer Science from Bharathiar University, Coimbatore. She is currently pursing her Ph.D under Avinashilingam Institute for Home Science & Higher Education for Women, Deemed University in Coimbatore. She has 13 years of teaching experience. Her area of interest is data mining and Web Designing. She has attended, organized seminars, research conventions and conferences in the field of computer science.

M. Thilagu is qualified with MCA.,M. Phil.Ph.D, SET in computer science. She has 22 years of teacher experience and 3 years of industrial experience. She is specializing in the areas of data mining, data analytics, text mining and NLP.She has published research articles in the reputed journals and conferences and book chapters. She is an invited resource person on talks relating to data analytics. She is currently guiding PhD research scholars and carrying out funded projects in interdisciplinary fields. She has attended and organized conferences, workshops and seminar to share and gain knowledge in the field of computer science.